Raman Scattering and Infrared Spectroscopy of Chemically Substituted Sr_2LnTaO_6 (Ln = Lanthanides, Y, and In) Double Perovskites

Anderson Dias,*,† L. Abdul Khalam,‡ Mailadil Thomas Sebastian,‡ Márcio Martins Lage,§ Franklin Massami Matinaga,§ and Roberto Luiz Moreira§

Departamento de Química, Universidade Federal de Ouro Preto, Campus Morro do Cruzeiro, ICEB II, Ouro Preto-MG, 35400-000, Brazil, Materials and Minerals Division, National Institute for Interdisciplinary Science and Technology, Trivandrum-695 019, India, and Departamento de Física, Universidade Federal de Minas Gerais, C.P. 702, Belo Horizonte-MG, 30123-970, Brazil

Received April 4, 2008. Revised Manuscript Received June 4, 2008

Sr_2LnTaO_6 (Ln = lanthanides, Y, and In) ceramics were prepared by a solid-state route, and their vibrational phonon modes were investigated using Raman and infrared (IR) spectroscopic techniques. Lorentzian lines were used to fit the Raman spectra, which showed 24 bands in perfect agreement with theoretical calculations. The IR spectra were fitted with a four-parameter semiquantum model, and the results showed 17 bands for the materials. The position and width of the phonon modes were determined and correlated to the ionic radii for the different atoms substituted in the B′-site. It was verified that all materials belong to the monoclinic $P2_1/n$ (C_{2h}^5) structure.

Introduction

It is well-known that ceramics with a perovskite structure represent potential compounds for technological applications.[1] These materials show an incredibly high versatility due to their wide array of structures and phases with totally different functions, which are directly related to the combination of chemical elements in the basic formula ABX_3. Multiple ion substitution in the perovskite lattice creates the so-called complex perovskites, which present pairs of unlikely valence cations in proportions depending on their oxidation states and ionic radii.[1] In the last 50 years, many compounds were studied in the framework of their crystal chemistry toward emerging applications: ferroelectrics,[2] superconductors,[3] relaxors,[4] photonics,[5] catalysts,[6] and microwave (MW) dielectrics.[7] The ever-growing proliferation in telecommunication technologies provided an increasing demand for MW dielectric ceramics.[7,8] These materials constitute the basic components in various communication and MW systems providing very effective size reduction for MW components. High dielectric constants (ε_r), minimum possible dielectric losses, and near-zero temperature stability of the resonant frequency (τ_f) are the basic requirements for MW applications, which are not fully attained by any compound. Even though a number of MW resonator materials are available, the demand for new MW dielectrics with a multifunctionality feature is also increasing.[7]

In this respect, complex perovskites provide a wide and good range of suitable materials due to the possibilities of tailoring the chemistry and consequently the parameters to meet device requirements. It is well-known that the final properties are highly dependent on the nature of the cations present as well as on structural features, including ordering and defects.[9] Extensive research was carried out to investigate the properties of complex $A(B'_{1/3}B''_{2/3})O_3$ perovskites, such as $Ba(Mg_{1/3}Ta_{2/3})O_3$ and $Ba(Zn_{1/3}Ta_{2/3})O_3$, as they possess excellent MW properties.[10] In spite of that, less attention has been paid to MW dielectric properties of $A_2B'B''O_6$, known as double perovskites. Current investigations on these ceramics showed a number of temperature-stable MW dielectric materials with potential new applications extending to the millimeter wave range.[11–14] Among the double perovskites recently investigated, the series containing lanthanides in the B-sites besides niobium or tantalum presented excellent MW properties.[11–14] For these ceramics, the crystal structures are controversial: cubic, pseudo-cubic, tetragonal,

* Corresponding author. Tel.: 55-31-3559-1716. E-mail: anderson_dias@iceb.ufop.br.
† Universidade Federal de Ouro Preto.
‡ National Institute for Interdisciplinary Science and Technology.
§ Universidade Federal de Minas Gerais.

(1) (a) Mitchell, R. H. *Perovskites: Modern and Ancient*; Almaz Press: Ontario, Canada, 2002. (b) *Properties and Applications of Perovskite Type Oxides*; Tejuca, L. G., Fierro, J. L. G., Eds.; Marcel Decker: New York, 1993.
(2) Samara, G. A. *J. Phys.: Condens. Matter.* **2003**, *15*, 367.
(3) Blackstead, H. A.; Dow, J. D.; Harshman, D. R.; Yelon, W. B.; Chen, M. X.; Wu, M. K.; Chen, D. Y.; Chien, F. Z.; Pulling, D. B. *Phys. Rev. B: Condens. Matter Mater. Phys.* **2001**, *61*, 214412-1.
(4) Bokov, A. A.; Ye, Z. G. *J. Mater. Sci.* **2006**, *41*, 31.
(5) Wojtowicz, A. J.; Drozdowski, W.; Wisniewski, D.; Lefaucheur, J. L.; Galazka, Z.; Gou, Z. H.; Lukasiewicz, T.; Kisielewski, J. *Opt. Mater.* **2006**, *28*, 85.
(6) Osterloh, F. E. *Chem. Mater.* **2008**, *20*, 35.
(7) Reaney, I. M.; Iddles, D. *J. Am. Ceram. Soc.* **2006**, *89*, 2063.
(8) Subodh, G.; James, J.; Sebastian, M. T.; Paniago, R.; Dias, A.; Moreira, R. L. *Chem. Mater.* **2007**, *19*, 4077.
(9) Knapp, M. C.; Woodward, P. M. *J. Solid State Chem.* **2006**, *179*, 1076.
(10) Varma, M. R.; Raghunandan, R.; Sebastian, M. T. *Jpn. J. Appl. Phys.* **2005**, *44*, 298.
(11) Khalam, L. A.; Sebastian, M. T. *Int. J. Appl. Ceram. Technol.* **2006**, *3*, 364.
(12) Khalam, L. A.; Sebastian, M. T. *J. Am. Ceram. Soc.* **2007**, *90*, 1467.
(13) Subodh, G.; Sebastian, M. T. *J. Am. Ceram. Soc.* **2007**, *90*, 2266.
(14) Dias, A.; Khalam, L. A.; Sebastian, M. T.; Paschoal, C. W. A.; Moreira, R. L. *Chem. Mater.* **2006**, *18*, 214.

10.1021/cm800969m CCC: $40.75
Published on Web 07/22/2008

orthorhombic, and monoclinic structures are frequently found in the literature.

Our group studied the crystal structures of complex perovskites using Raman and infrared (IR) spectroscopies.[14–17] These techniques are employed to investigate the behavior of the polar phonon modes, which represent the intrinsic dielectric contributions to the MW response and are directly dependent on the crystalline structure. Thus, to study the potential of a given material to MW applications (resonators or filters), the knowledge of its polar phonon features is mandatory. Barium-,[17] strontium-,[18] and calcium-based[12] complex perovskites with lanthanides previously were studied from the point-of-view of their MW dielectric properties, but only the ceramics containing Ba were investigated by spectroscopic techniques,[14,17] although a preliminary incomplete study on Sr-based ceramics was published some years ago.[19] For these materials, cubic, tetragonal, and orthorhombic structures were reported for the lanthanide series depending on the ionic radii.[18,19] In this work, the vibrational properties of Sr_2LnTaO_6 ceramics (Ln = lanthanides, Y, and In) were investigated in detail by Raman scattering and far-IR spectroscopy together with group-theory calculations. The results showed correlations between structures and vibrational modes for these materials, allowing us to contribute to the debate on the crystalline structure of this lanthanide series.

Experimental Procedures

Sr_2LnTaO_6 (Ln = La, Pr, Nd, Sm, Eu, Gd, Tb, Dy, Ho, Er, Yb, Y, and In) ceramics were prepared by a solid-state ceramic route. High-purity $SrCO_3$ (99.9%, Aldrich Chemical, St. Louis, MO), rare-earth oxides (99.99%, Treibacher, Althofen, Austria), and Ta_2O_5 (99.9%, Nuclear Fuel Complex, Hyderabad, India) were used as the starting materials. Stoichiometric amounts of powder mixtures were ball-milled in a distilled water medium using yttria-stabilized zirconia balls in a plastic container for 48 h. The slurry was dried, ground well, and calcined at 1250 °C for 4 h. Because of the poor sinterability of the ceramics with Ho and Y, 0.5 wt % Nb_2O_5 was added as a sintering aid and mixed thoroughly with the powders in distilled water and dried. They were then mixed with 3 wt % polyvinyl alcohol (molecular weight ≈ 22 000, BDH Laboratory Suppliers) and again dried and ground well. Cylindrical pucks of ~7−9 mm in height and 14 mm in diameter were produced by applying a pressure of 150 MPa. These compacts were then fired at 600 °C for 30 min to expel the binder before being sintered at 1600 °C for 4 h. Bulk densities of the sintered samples were measured using Archimedes' method, and the results showed ceramics with values in the range of 97−99% of the theoretical value.[18]

The crystal structure and phase purity of the powdered samples were studied by X-ray diffraction (XRD) using Cu Kα radiation (λ = 0.15418 nm) in a Rigaku diffractometer, with a graphite monochromator and a nickel filter in the 2θ range of 10−140° (step 0.02°2θ). Raman spectra were collected in a back-scattering configuration by using an Olympus confocal microscope attached to a triple-monochromator T64000 Jobin-Yvon spectrometer (objective 50×). The 532 nm line of the YVO_4:Nd laser (second harmonic line with an output of 3 mW at the sample's surface) together with two different lines of an Ar^+ laser (514.5 and 488 nm with effective 2 mW power at the sample's surface) were used as the exciting lines. A liquid N_2-cooled charge coupled device (CCD) detected the scattered light. The frequency resolution was better than 2 cm^{-1}, and the accumulation times were typically five collections of 60 s. The obtained spectra were divided by the Bose−Einstein thermal factor[20] before being fitted by a sum of Lorentzian lines. IR reflectivity spectra were recorded in a Fourier-transform spectrometer (Bomem DA 8-02) equipped with a fixed-angle specular reflectance accessory (external incidence angle of 11.5°). In the mid-IR region (500−4000 cm^{-1}), we used a SiC glow-bar lamp as the IR source, a Ge-coated KBr beamsplitter, and a liquid N_2-cooled HgCdTe detector. In the far-IR range (50−600 cm^{-1}), we employed a mercury-arc lamp, a 6 μm coated Mylar hypersplitter, and a liquid He-cooled Si bolometer. The sample surfaces were polished to an optical grade (0.25 μm) before measurements. A gold mirror was used as a reference. The data were collected at a pressure of 10^{-4} bar and a frequency resolution of 2 cm^{-1}. The reflectivity spectra were evaluated by means of standard Kramers−Krönig analysis and adjusted by an oscillator model. A generalized four-parameter oscillator model was used rather than the classical model to achieve a good fit with a minimum number of physically meaningful oscillators.

Results

Figure 1 presents the XRD analysis of sintered Sr_2LnTaO_6 ceramics, which are quite similar and dominated by the strong lines characteristic of a primitive cubic unit cell. A number of weak additional lines, indicative of the presence of a supercell, in all compounds also were visible. Close examination showed superlattice reflections in all samples, particularly at $2\theta \approx 18°$ (marked by an asterisk in Figure 1 for the Gd sample), confirming an ordered arrangement between Ln and Ta ions in the B-site sublattice. According to Fu and Ijdo,[21] these reflections are a consequence of the antiphase tilting (−) of the octahedra around the principal 2-fold $[110]_p$-axis. Also, other reflections, such as that located at $2\theta \approx 24°$ (marked with an arrow in Figure 1 for the sample containing Gd), arising from an in-phase tilt of the octahedra around the primitive axis are denoted.[21] Similar results also were observed by Kanaiwa et al.,[22] who studied the same ceramic system by using Rietveld procedures and concluded for the monoclinic structure space group $P2_1/n$. Fu and Ijdo[21] studied Sr_2InSbO_6 and Sr_2YSbO_6 compounds by XRD and neutron powder diffraction and reported a monoclinic distortion for these materials. Ting et al.[23] investigated Sr_2InNbO_6 materials by neutron and electron diffraction techniques and concluded a monoclinic structure, discarding both tetragonal and orthorhombic symmetries, although the authors recognized that the monoclinic distortion is fairly small.[21,23] In

(15) Surendran, K. P.; Sebastian, M. T.; Mohanan, P.; Moreira, R. L.; Dias, A. *Chem. Mater.* **2005**, *17*, 142.
(16) Dias, A.; Matinaga, F. M.; Moreira, R. L. *Chem. Mater.* **2007**, *19*, 2335.
(17) Moreira, R. L.; Khalam, L. A.; Sebastian, M. T.; Dias, A. *J. Eur. Ceram. Soc.* **2007**, *27*, 2803.
(18) Khalam, L. A.; Sebastian, M. T. *J. Am. Ceram. Soc.* **2006**, *89*, 3689.
(19) Ratheesh, R.; Wöhlecke, M.; Berge, B.; Wahlbrink, T.; Haeuseler, H.; Ruhl, E.; Blachnik, R.; Balan, P.; Santha, N.; Sebastian, M. T. *J. Appl. Phys.* **2000**, *88*, 2813.
(20) Hayes, W.; Loudon, R. *Scattering of Light by Crystals*; Wiley: New York, 1978.
(21) Fu, W. T.; Ijdo, D. J. W. *Solid State Commun.* **2005**, *134*, 177.
(22) Kanaiwa, Y.; Wakeshima, M.; Hinatsu, Y. *Mater. Res. Bull.* **2002**, *37*, 1825.
(23) Ting, V.; Liu, Y.; Withers, R. L.; Krausz, E. *J. Solid State Chem.* **2004**, *177*, 979.

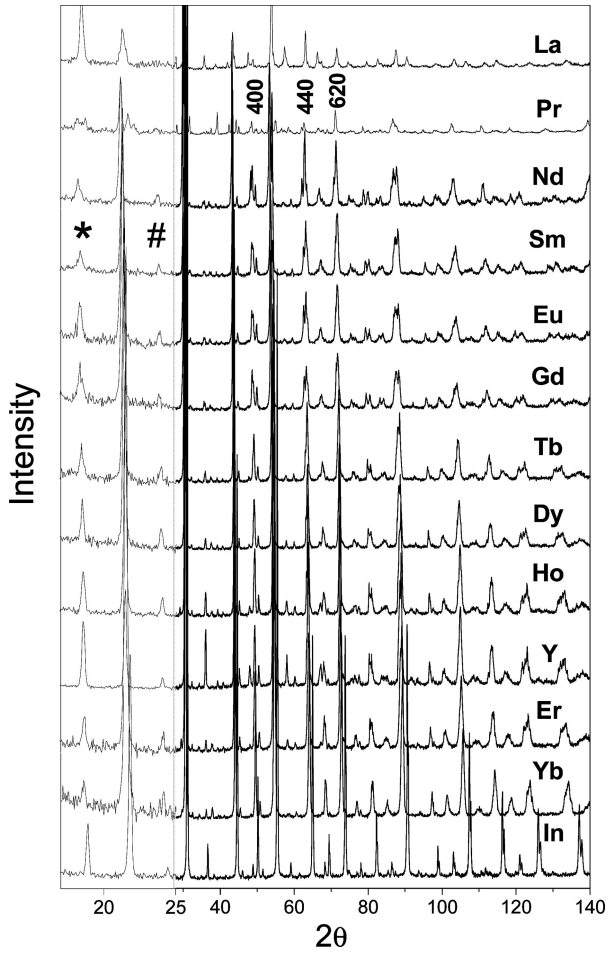

Figure 1. XRD for all Sr_2LnTaO_6 (Ln = lanthanides, Y, and In) materials studied. A superlattice reflection due to negative tilts around the principal $[110]_p$-axis is marked with an asterisk, while superlattice diffractions arising from an in-phase tilt of the octahedra are indicated by the symbol #. The dashed line denotes a change in the intensity scale used for better visualization of the range of 17−25°2θ.

the present work, it was observed that as the ionic radii of the Ln elements increase (from In to La), the reflection peaks shift toward the low-angle (higher lattice parameter) side. A significant shift of the peaks for the In sample toward higher angles when compared to the peaks of the lanthanides and yttrium ceramics can be attributed to the large difference in their ionic radii. The splitting of the group of reflections indexing as (400), (440), and (620) indicates a symmetry lower than tetragonal for all materials, in contrast to the results for Ba-based ceramics previously published by Dias et al.[14] In view of that, the structure of this Sr-based lanthanide series was investigated by Raman and IR spectroscopies together with group-theory calculations.

Room-temperature Raman analysis was carried out in all Sr_2LnTaO_6 materials, and the results are displayed in Figure 2. As can be seen, similar spectral profiles are clearly observed, which indicates that the ceramics likely occur in the same crystalline structure. Dominating bands located at 100−200, 420, and 800 cm^{-1} are present in the samples, which were previously observed in similar 1:1 ordered ceramics.[14,17] The sharp and intense set of bands in the range of 100−200 cm^{-1} remains the main feature of the tetragonal structure previously verified in Ba-based ceramics with lanthanides,[14] but the observed splitting is clear evidence

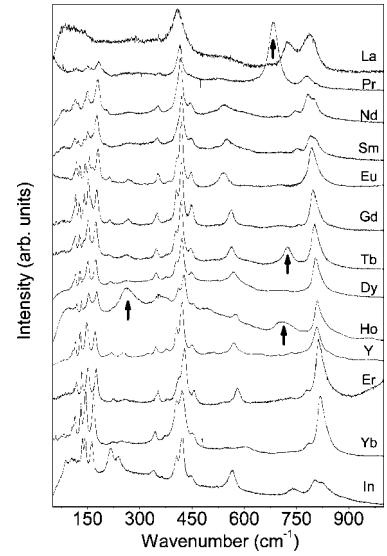

Figure 2. Room-temperature Raman spectra for Sr_2LnTaO_6 (Ln = lanthanides, Y, and In) complex perovskites. Extra bands due to mixed oxidation states are marked with arrows in samples containing Pr, Tb, and Ho.

for a lowering in the tetragonal symmetry, as will be discussed later. For samples containing La, Eu, Ho, and Er, the 488 nm exciting line was used to avoid the extra bands observed when using 514 and 532 nm as laser lines. In this respect, the samples with Pr, Tb, and even Ho presented extra bands (marked with arrows in Figure 2) probably related to mixed oxidation states (i.e., reagents Pr_6O_{11} and Tb_4O_7 were employed), which could not be removed or avoided by changing the excitation line. Because of the large number of modes, the detailed assignment could be achieved only with the help of lattice dynamical calculations. To perform such calculations, it is necessary to know the symmetries of the vibrational modes from the polarized spectra of a single crystal. Unfortunately, single crystals are not available, and therefore, it is not possible to obtain a reliable assignment of all modes observed. Thus, the assignment was performed by comparing experimental data with other complex perovskites.

As a general trend, the Raman bands of all Sr_2LnTaO_6 ceramics are up-shifted (from La to In), which is a consequence of the smaller In ions as compared to La ions, leading to a contracted unit cell with smaller ionic distances and then to stronger ionic bonds. Practically no variation in frequency was observed for bands below 600 cm^{-1}, which are related to Sr ($A_g \oplus B_g$ cubic-like modes) and Sr−O (A_g) vibrations (translational motions) and are insensitive to chemical substitution on B-sites. While the mode centered at 530−570 cm^{-1} can be assigned as the B_g stretching mode (ν_2 for a free octahedron), the set of modes centered at 410−420 cm^{-1} corresponds to the bending modes (ν_5 for a free octahedron). The region below 300 cm^{-1} is normally affected by composition (external modes), but no change was observed, probably due to invariance of the cation on the B″-site (Ta) in the samples studied. For frequencies above 600 cm^{-1}, a shift to lower frequencies was detected as a function of the rare-earth ion, from In to La, as commented previously. The frequency range of 650−950 cm^{-1} represents vibrations of the oxygen octahedra with Ln/Ta cations

on their interior. Changes in the composition affect the modes, especially the A_g(O) peaks at 790−830 cm^{-1} (totally symmetric stretching of TaO_6 octahedra or ν_1 mode for a free octahedron).

The Raman spectra of the ceramic containing La must be discussed separately. As can be seen in Figure 2, the splitting of the F_{2g}(1)-like mode is not clear, albeit our efforts to obtain good Raman data, including different laser lines, intensities, and acquisition times. Ratheesh et al.[19] studied these ceramics and verified remarkable changes in their MW properties as compared to other lanthanides. Although the tolerance factor for this sample indicates a strong deviation from cubic symmetry, the Raman experimental data are not consistent with this auxiliary parameter. In terms of ionic radii, Sr^{2+} and La^{3+} exhibit (coordination number 12) very close values: 1.58 and 1.50 Å, respectively. It is then possible that a partial intersubstitution occurred between the A-site occupied by Sr ions and the B-site occupied by La ions. However, the width of the broadband at 100−200 cm^{-1} is comparable to the corresponding bands in the other rare-earth, Y, and In ceramics, displayed in Figure 2. From these observations, it is not possible to conclude possible intersubstitutions in this La containing ceramic.

The ideal simple perovskite is cubic, space group $Pm\bar{3}m$, which presents no-active first-order Raman phonons and only three IR-active modes. For complex cubic perovskites of general formula $A_2B'B''O_6$, $Fm\bar{3}m$ symmetry (O_h^5, No. 225, Glazer's notation $a^0a^0a^0$) is frequently expected in ordered untilted lattices. This configuration allows classification of the normal modes at the Brillouin zone center as $\Gamma = A_{1g} \oplus E_g \oplus F_{1g} \oplus 2F_{2g} \oplus 5F_{1u} \oplus F_{2u}$.[14] Symmetry analysis of the irreducible representations indicates that four modes are Raman-active (A_{1g}, E_g, and $2F_{2g}$) and also that four modes are IR-active ($4F_{1u}$). The strong features observed in Figure 2 can be assigned to these first-order Raman active modes; however, many additional features appeared, particularly in the triply degenerate low-frequency F_{2g}(1) mode. The sharp and intense lines in the range of 100−200 cm^{-1} split into at least four bands, which lead us to investigate the crystal structure of this lanthanide series. Literature data and previous results with Ba-based, lanthanide ceramics indicate that a structure with a symmetry lower than tetragonal is more plausible for these materials; in particular, the monoclinic $P2_1/n$ structure.[21−25] Because of the completely different Raman patterns observed for Ba-based materials and our present samples,[14,26] in the absence of clear splitting of the triply degenerate mode in the 100−200 cm^{-1} region, the hypothesis for an orthorhombic structure was disregarded.

Thus, we adopted the much more common tetragonal structure for this type of ordered double perovskite ($I4/m$, No. 87, C_{4h}^5 space group).[27] This tetragonal structure is derived from the prototype $Fm\bar{3}m$ cubic structure by a single rotation (antiphase) of the LnO_6 and TaO_6 octahedra along the [001] direction of the cubic cell (Glazer's notation $a^0a^0c^-$). For this structure, the Sr atoms occupy 4d sites of S_4 symmetry, the Ln and Ta ions occupy 2a and 2b sites of C_{4h} symmetry, and the oxygen atoms are in the 8h and 4e sites (C_s and C_4 symmetries, respectively). Then, using the site-group method of Rousseau et al.,[28] it is possible to obtain the following distribution in terms of the irreducible representations of the C_{4h} point group: $\Gamma = 3A_g \oplus 5A_u \oplus 3B_g \oplus B_u \oplus 3E_g \oplus 6E_u$. Excluding the acoustic ($A_u \oplus E_u$) and silent modes (B_u), we would expect nine Raman-active modes ($3A_g$, $3B_g$, and $3E_g$) and nine IR bands ($4A_u$ and $5B_u$) for this structure. As can be easily observed in Figures 2 and 3, the number of Raman and IR bands is higher than nine, which means that the symmetry of our ceramics is lower than the tetragonal space group $I4/m$. Also, XRD results showed that both antiphase and in-phase tilts occur in these materials, which do not allow this particular tetragonal structure. The only possibility for a tetragonal structure with in-phase and antiphase tilts ($P4_2/n$, No. 86, $a^+a^+c^-$)[29] predicts 35 Raman-active bands and another 35 IR-active modes, which is not compatible with our experimental data.

We assume a monoclinic structure, space group $P2_1/n$ (C_{2h}^5, No. 14, Glazer's notation $a^-a^-c^+$), which can be understood to result from a combination of in-phase (+) and antiphase (−) tilts of LnO_6 and TaO_6 octahedra in the (− − +) sense around the <001> axes of the ideal cubic perovskite. This structure presents a direct group−subgroup relationship with tetragonal $I4/m$ symmetry, discussed previously.[29] In this case, Ln and Ta ions should occupy the 2a and 2b Wyckoff-sites of both C_i symmetry, and Sr and O ions are in 4e sites of general C_1 symmetry. The site-group method[28] leads now to the following distribution of irreducible representations of the C_{2h} point group: $\Gamma = 12A_g \oplus 12B_g \oplus 18A_u \oplus 18B_u$. Thus, one would have 24 Raman-active phonon modes ($12A_g$ and $12B_g$) and 33 IR-active modes ($17A_u$ and $16B_u$) for these samples (the acoustic modes are $A_u \oplus 2B_u$). On the basis of the previous factor-group analyses, careful fittings of the Raman spectra were carried out, and the results for a typical sample are displayed in Figure 3. As an example, the spectrum for the ceramic containing Gd was divided into three wavenumber regions for better visualization: 30−310, 290−650, and 640−1005 cm^{-1} (Figure 3a−c). The final fittings (red lines in Figure 3) were obtained through a sum of 24 Lorentzian lines, in perfect agreement with the previous theoretical predictions (similar fittings with 24 bands could be obtained for all other ceramics). Table 1 presents the parameters after deconvolution of the spectrum of Sr_2GdTaO_6 (i.e., wavenumbers (cm^{-1}) and full width at half-maximum (cm^{-1})) for the phonon modes identified by experimental data. The present Raman spectroscopic results lead us to conclude that the correct structure for the Sr_2LnTaO_6 perovskites appears to be within the monoclinic $P2_1/n$ (C_{2h}^5) structure.

(24) Ting, V.; Liu, Y.; Withers, R. L.; Norén, L.; James, M.; Fitzgerald, J. D. *J. Solid State Chem.* **2006**, *179*, 551.
(25) Howard, C. J.; Barnes, P. W.; Kennedy, B. J.; Woodward, P. M. *Acta Crystallogr., Sect. B: Struct. Sci.* **2005**, *61*, 258.
(26) Dias, A.; Khalam, L. A.; Sebastian, M. T.; Moreira, R. L. *J. Solid State Chem.* **2007**, *180*, 2143.
(27) Lufaso, M. W.; Barnes, P. W.; Woodward, P. M. *Acta Crystallogr., Sect. B: Struct. Sci.* **2006**, *62*, 397.
(28) Rousseau, D. L.; Bauman, R. P.; Porto, S. P. S. *J. Raman Spectrosc.* **1981**, *10*, 253.
(29) Howard, C. J.; Kennedy, B. J.; Woodward, P. M. *Acta Crystallogr., Sect. B: Struct. Sci.* **2003**, *59*, 463.

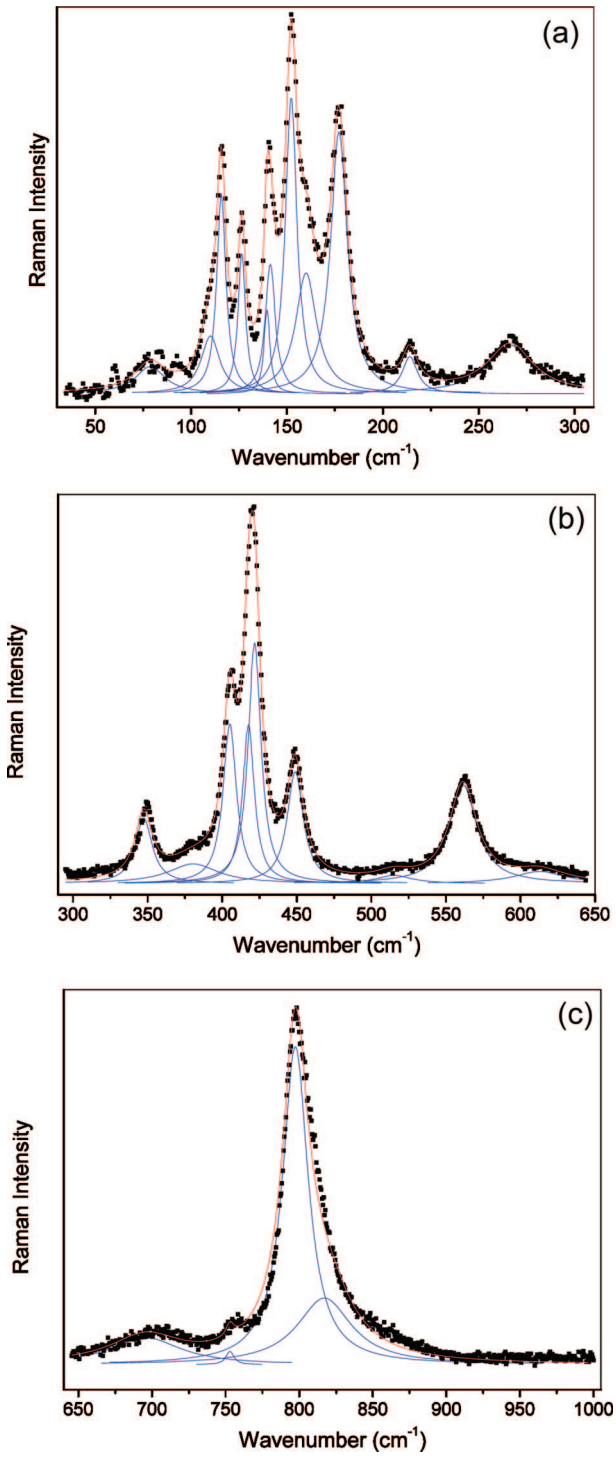

Figure 3. Raman spectra for Sr_2GdTaO_6 ceramics: (a) 50−300 cm^{-1}, (b) 300−600 cm^{-1}, and (c) 600−900 cm^{-1}. Experimental data are solid squares, while the fitting curve is the red line. Blue lines represent phonon modes adjusted by Lorentzian curves.

Table 1. Observed Raman Modes for Sr_2GdTaO_6 Ceramics[a]

band	Ω	γ
1	79.5	19
2	110.4	12
3	116.1	6
4	126.7	5
5	139.8	4
6	141.5	6
7	152.3	7
8	160.1	13
9	177.2	11
10	214.3	10
11	267.3	29
12	348.7	13
13	381.2	40
14	405.4	11
15	417.8	9
16	421.9	10
17	448.9	13
18	562.0	22
19	515.2	29
20	614.3	42
21	798.7	21
22	698.4	56
23	754.6	7
24	818.4	45

[a] Positions (Ω, cm^{-1}) and full width at half-maximum (γ, cm^{-1}) were obtained from adjustment of experimental data by Lorentzian lines.

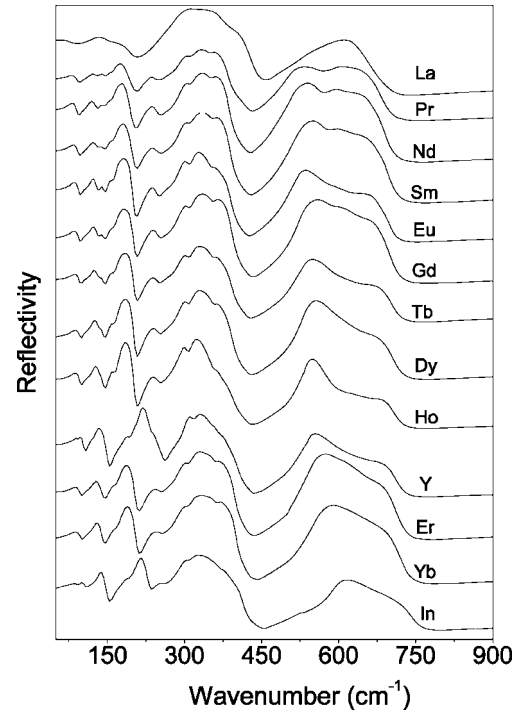

Figure 4. IR spectra for Sr_2LnTaO_6 (Ln = lanthanides, Y, and In) materials.

The IR reflectivity spectra of all samples studied in the present work are displayed in Figure 4. Visual inspection of the spectra shows at least 10 well-defined modes for all materials. Notice the high similarity between the spectra of the ceramics with different Ln ions, confirming their average noncubic symmetry, as will be discussed later. Again, the higher number of bands if compared to tetragonal ceramics previously studied[14] also indicates a lower symmetry than the common tetragonal. As a preliminary assignment, the bands above 450 cm^{-1} contain the ν_3 (F_{1u}) modes for a free octahedron, while the 300−450 cm^{-1} region includes the bending ν_4 modes. Below 300 cm^{-1}, the external (translational) modes dominate. Careful inspection of Figure 4 reveals the presence of many strong and weak bands, as well as shoulders in all samples. In view of that, a group-theory investigation was undertaken toward a better understanding of the crystal chemistry of these materials. The exact number of bands will be known only after precise fitting by using the four-parameter semiquantum model[30] and a nonlinear least-squares program.[31] According to this model, the IR

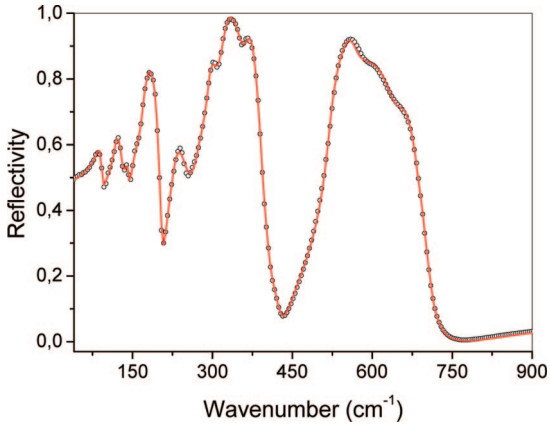

Figure 5. IR spectrum for Sr_2GdTaO_6 sample. Experimental data in open circles were fit by using the four-parameter semiquantum model (solid red line).

Table 2. Dispersion Parameters Calculated from Fit of IR Reflectance Spectrum of Sr_2GdTaO_6[a]

$\Omega_{j,TO}$	$\gamma_{j,TO}$	$\Omega_{j,LO}$	$\gamma_{j,LO}$	$\Delta\varepsilon_j$	$10^5 \tan\delta_j/\omega$
90.1	11.4	93.6	9.4	3.744	17.768
110.1	38.9	113.2	25.8	3.370	36.634
121.0	14.0	133.4	14.3	5.013	16.215
139.4	17.0	140.8	48.9	0.255	0.756
144.0	13.2	144.5	7.3	0.091	0.196
173.9	11.8	204.3	11.9	6.905	9.157
231.6	23.9	255.2	43.8	2.645	3.998
278.3	29.0	292.9	39.9	2.061	2.612
293.1	14.4	306.4	43.3	0.020	0.011
317.0	26.3	362.2	39.4	0.817	0.724
364.3	29.9	398.1	46.6	0.048	0.036
399.2	47.6	400.6	37.4	0.001	0.001
426.9	47.3	428.0	28.9	0.014	0.012
520.6	21.9	567.0	39.2	1.540	0.422
567.0	45.6	644.3	48.2	0.001	0.001
647.6	46.2	689.6	41.4	0.013	0.005
693.6	47.2	704.7	27.2	0.003	0.001
$\varepsilon_\infty = 3.703$		$\varepsilon_r = 30.244$		$\Sigma \tan\delta_j/\omega = 86.4 \times 10^{-5}$	

[a] Positions (Ω) and damping constants (γ) are given in cm^{-1}.

phonon contributions to the complex dielectric function $\varepsilon(\omega)$ are given by[30]

$$\varepsilon(\omega) = \varepsilon_\infty \prod_{j=1}^{N} \frac{\Omega_{j,LO}^2 - \omega^2 + i\omega\gamma_{j,LO}}{\Omega_{j,TO}^2 - \omega^2 + i\omega\gamma_{j,TO}} \quad (1)$$

where ε_∞ is the dielectric constant due to the electronic polarization contribution, and $\Omega_{j,LO}(\Omega_{j,TO})$ and $\gamma_{j,LO}(\gamma_{j,TO})$ are the frequency and damping of the j-th longitudinal (transverse) optical modes, respectively. N is the number of polar phonons. At quasi-normal incidence, the dielectric function is related to the optical reflectance R by the Fresnel formula

$$R = \left| \frac{\sqrt{\varepsilon(\omega)} - 1}{\sqrt{\varepsilon(\omega)} + 1} \right|^2 \quad (2)$$

Eqs 1and 2were used to fit the experimental data for the Gd ceramic (chosen as a typical sample), and the results are presented in Figure 5 as a solid red curve. Then, we obtained the wavenumbers and widths of the transverse (TO) and longitudinal (LO) IR modes, which are listed in Table 2 for this sample. We note first that 17 IR modes could be adjusted for the Sr_2GdTaO_6 ceramic, which is quite similar to the situation found for $RE_2MgB''O_6$ (RE = rare earth and B'' = Ti, Sn) compounds. For these materials, quasi-accidental degeneracy forbids distinction between corresponding A_u and B_u modes, and also only 17 IR modes were observed instead of the 33 foreseen ones ($17A_u$ and $16B_u$).[32–34] The resemblance of the spectra of our Sr_2GdTaO_6 compound and those of $RE_2MgB''O_6$,[32–34]which is derived from the fact that the vibrational modes come essentially from the MgO_6 and $B''O_6$ octahedra, are tentatively assigned in refs 32–34.

Once the IR modes were determined, the oscillator strengths of the individual j-th TO modes were obtained (Table 2) by[30]

$$\Delta\varepsilon_j = \frac{\varepsilon_\infty}{\Omega_{j,TO}^2} \frac{\prod_k (\Omega_{k,LO}^2 - \Omega_{j,TO}^2)}{\prod_{k\neq j} (\Omega_{k,TO}^2 - \Omega_{j,TO}^2)} \quad (3)$$

Now, the static (IR) dielectric constant, which corresponds to the intrinsic MW dielectric constant, can be obtained by adding the oscillator strengths over all modes according to

$$\varepsilon_r = \varepsilon_\infty + \sum_{j=i}^{N} \Delta\varepsilon_j \quad (4)$$

The values of ε_r and ε_∞ for the sample with Gd are given in Table 2, together with the phonon modes. It is important to note that the intrinsic unloaded quality factor at the MW region, Q_u, can be calculated as the reciprocal of the dielectric loss tangent ($\tan\delta$) in the limit where $\Omega_{j,TO} \gg \omega$, which leads to the equation

$$\tan\delta = \sum_j \tan\delta_j = \sum_j \omega \frac{\Delta\varepsilon_j \gamma_{j,TO}}{\varepsilon_r \Omega_{j,TO}^2} \quad (5)$$

The values for $\sum_j \tan\delta_j/\omega$ are also in Table 2. The value of the intrinsic (FTIR) quality factor time frequency was 35 THz for Gd containing ceramics. This value is 1 order of magnitude larger than the MW samples[18] because the extrapolation of IR losses to the MW region is often spoiled due to the dominance of extrinsic losses of different origins (polar species, microstructural defects, etc.) leading to overestimated FTIR quality factors.[35–37] The lower value is also due to the fewer number of modes depicted by fitting because of the proximity between modes of different irreducible representations, which forbids their individual assessment by regular fitting procedures. Intrinsic ε_r is in good agreement with the previously published MW measurements.[18]

The IR reflectance spectra displayed in Figure 4 were subjected to Kramers−Krönig analysis. The complex dielectric constant, $\varepsilon(\omega) = \varepsilon'(\omega) + I\varepsilon''(\omega)$, of each Sr_2LnTaO_6

(30) Gervais, F.; Echegut, P. In *Incommensurate Phases in Dielectrics*; Blinc, A., Levanyuk, A. P., Eds.; North Holland: Amsterdam, 1986; p 337.
(31) Meneses, D. D.; Gruener, G.; Malki, M.; Echegut, P. *J. Non-Cryst. Solids* **2005**, *351*, 124.
(32) Salak, A. N.; Khalyavin, D. D.; Ferreira, V. M.; Ribeiro, J. L.; Vieira, L. G. *J. Appl. Phys.* **2006**, *99*, 94104.
(33) Babu, G. S.; Subramanian, V.; Murthy, V. R. K.; Lin, I. N.; Chia, C. T.; Liu, H. L. *J. Appl. Phys.* **2007**, *102*, 64906.
(34) Babu, G. S.; Subramanian, V.; Murthy, V. R. K.; Moreira, R. L.; Lobo, R. P. S. M. *J. Appl. Phys.* **2008**, *103*, 84104.
(35) Petzelt, J.; Kamba, S. *Mater. Chem. Phys.* **2003**, *79*, 175.
(36) Zurmühlen, R.; Petzelt, J.; Kamba, S.; Voitsekhovskii, V.; Colla, E.; Setter, N. *J. Appl. Phys.* **1995**, *77*, 5341.
(37) Zurmühlen, R.; Petzelt, J.; Kamba, S.; Kozlov, G.; Volkov, A.; Gorshunov, B.; Dube, D.; Tagantsev, A.; Setter, N. *J. Appl. Phys.* **1995**, *77*, 5351.

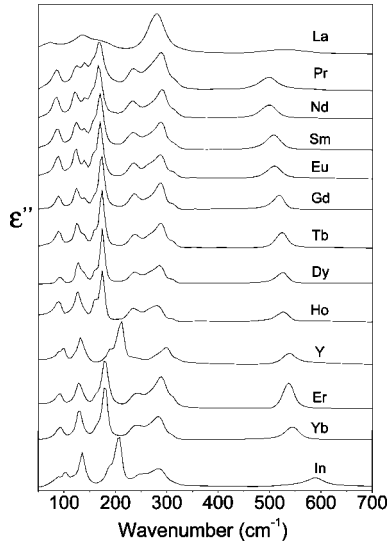

Figure 6. Imaginary part of dielectric constant (ε'') calculated from Kramers−Krönig analysis for Sr_2LnTaO_6 ceramics in the far-IR region (50−700 cm^{-1}).

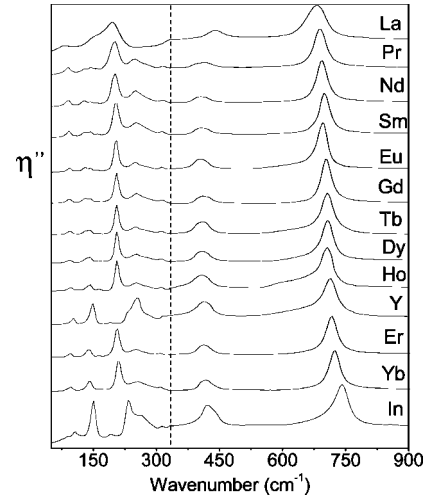

Figure 7. Inverse of the imaginary part of the dielectric constant (η'') calculated from Kramers−Krönig analysis for all Sr_2LnTaO_6 materials in the far-IR region. The dashed line centered at 332 cm^{-1} denotes a change in the intensity scale used for better visualization.

material was calculated, and the imaginary parts of $\varepsilon(\omega)$ and $1/\varepsilon(\omega)$, denoted ε'' and η'', were analyzed in detail. These optical functions were studied because they give, respectively, the values of the TO and LO mode frequencies and damping constants. These values can be compared to those normally obtained from the fit with the advantage of studying individual phonon contributions without any physical inconsistency. Figures 6 and 7 show both ε'' and η'' as functions of the chemical substitution on the B-site of the double perovskite in the range of 50−900 cm^{-1}. Many distinct modes can be clearly seen in Figures 6 and 7, which varied in shape and intensity as the ion changed. The lower frequency modes in Figure 6 (<350 cm^{-1}) are the most important in view of their contribution to dielectric and MW properties. These set of intense peaks represent the main vibrational modes and can be attributed to the Sr-BO_3 external vibration as well as to the vibrations for each LnO_6 and TaO_6 octahedra (O-Ln-O and O-Ta-O bending). Because the charge of Ta^{5+} is higher than that of Ln^{3+}, the force constant associated with the Ta-O vibration must be larger than that of the Ln-O vibration. As a consequence, Ln-O modes dominate the lower frequency region of the spectra. Besides, higher Ln ionic radii (from In to La) lead to lower frequency modes. Similar behavior can be seen in vibrational modes in the range of 500−600 cm^{-1}, which are less intense, broader (larger damping), and downshifted with increasing Ln^{3+} ionic radii. Figure 7 (η'') supplies a good image of the evolution of these modes, especially above 400 cm^{-1}, which are related to the O-Ta-O bending (the dashed line is centered at 332 cm^{-1} and represents a change in the intensity scale used for better visualization). The most relevant information in the highest wavenumber range (600−900 cm^{-1}) concerns the contributions of TaO_6 and LnO_6 stretching vibrations to optical and dielectric properties. As a general trend, the frequency decreasing and broadening of the polar (IR) modes with Ln ionic radii explain, respectively, the observed increase of the dielectric constants and a decreasing tendency of quality factors at the MW region.[18]

Conclusion

Sr_2LnTaO_6 (Ln = lanthanides, Y, and In) ceramics were prepared with the aim of being applied as dielectric resonators in telecommunication systems. Together with the XRD technique, experimental Raman and IR data allowed us to determine the correct structure and phonon modes for all the lanthanide series in Sr-based double perovskites in light of group-theoretical models. A total of 24 Raman-active bands and 17 IR phonon modes were observed, in good agreement with group-theoretical calculations for a monoclinic $P2_1/n$ (C_{2h}^5) structure.

Acknowledgment. The Brazilian authors acknowledge financial support from CNPq, FINEP, and FAPEMIG. The Indian authors are grateful to the Council of Scientific and Industrial Research (India). Special thanks go to Alexandre M. Moreira for his assistance with XRD analyses.

CM800969M